33rd Annual International Conference of the IEEE EMBS
Boston, Massachusetts USA, August 30 - September 3, 2011

Brain Tissue Segmentation in PET-CT Images Using Probabilistic Atlas and Variational Bayes Inference

Yong Xia, *Member IEEE*, Jiabin Wang, Stefan Eberl, *Member IEEE*, Michael Fulham, and David Dagan Feng, *Fellow, IEEE*

***Abstract*—PET-CT provides aligned anatomical (CT) and functional (PET) images in a single scan, and has the potential to improve brain PET image segmentation, which can in turn improve quantitative clinical analyses. We propose a statistical segmentation algorithm that incorporates the prior anatomical knowledge represented by probabilistic brain atlas into the variational Bayes inference to delineate gray matter (GM), white matter (WM) and cerebrospinal fluid (CSF) in brain PET-CT images. Our approach adds an additional novel aspect by allowing voxels to have variable and adaptive prior probabilities of belonging to each class. We compared our algorithm to the segmentation approaches implemented in the expectation maximization segmentation (EMS) and statistical parametric mapping (SPM8) packages in 26 clinical cases. The results show that our algorithm improves the accuracy of brain PET-CT image segmentation.**

***Index Terms*- Brain image segmentation, PET-CT imaging, Gaussian mixed model, variational Bayes inference**

I. Introduction

Positron emission tomography (PET) can detect subtle functional changes at the early stages of a disease process, and hence offers advantages over anatomical imaging techniques in the early evaluation of neurodegenerative disorders [1]. An accurate quantitative analysis of brain PET images necessitates clear delineation of gray matter (GM), white matter (WM) and cerebrospinal fluid (CSF). Since manual segmentation of brain images is time consuming and highly subjective, a number of automated approaches have been proposed in the literature, including those based on the brain atlas [2, 3], statistical models [4, 5], deformable models [6] and Markov random field (MRF) models [7].

There are several tools which can register a brain PET image to an atlas and map brain structures from the atlas to the image [2, 3]. Normal anatomical variation across patients, however, limits the performance of such atlas-based joint registration-comparison segmentation. Statistical approaches [4, 5] assume brain voxel values to satisfy the Gaussian mixed model (GMM) with parameters estimated by the expectation maximization (EM) algorithm, and determine voxel class labels based on the maximum a posteriori (MAP) criterion. To advantage their complementary strengths, atlas-based approaches have been combined effectively with statistical techniques to improve segmentation accuracy. The segmentation algorithm [8] in the statistical parametric mapping (SPM8) [9] uses a modified cluster technique based on the GMM, where the prior likelihood of each voxel belonging to each brain structure is provided by a brain atlas.

Traditionally, brain tissue segmentation is based on magnetic resonance (MR) images, since these images yield high-contrast anatomical information. However, MR images provide little functional data and the delineation of neurodegenerative diseases on the basis of atrophy is problematic. PET-CT scanning has now replaced PET-only scanning in clinical practice. The PET-CT scanner combines a PET scanner and a fast helical computed tomography (CT) scanner in one instrument, thus the functional PET imaging is complemented by the co-registered anatomical CT imaging. The high resolution CT anatomical data offers the opportunity to improve the segmentation of brain structures in PET images. Potesil et al. [10] used both PET and CT information to calculate the joint-likelihood ratio for tumor delineation. In our previous work, we applied the spatial clustering technique [11] and MAP-MRF model [12] to segment brain PET-CT images. Recently, we investigated the automated weighting scheme [13] and classification fusion method [14] to use the PET and CT data jointly and adaptively.

In this paper, we propose a more accurate statistical segmentation approach called the probabilistic atlas-based variational EM (PA-VEM) algorithm for brain PET-CT images. In this algorithm, we revise the statistical model by enabling each voxel to have different prior probabilities, replace the maximum likelihood estimation with the variational Bayes inference [15], and use the probabilistic brain atlas to incorporate prior anatomical knowledge into the segmentation process. We compared our algorithm to the segmentation approaches in the EM segmentation (EMS) [16] and SPM8 packages in clinical studies.

Manuscript received April 15, 2011. This work was supported in part by the PolyU and ARC grants.

Y. Xia, J. Wang, S. Eberl, M. Fulham, and D. Feng are with the BMIT Research Group, School of Information Technologies, The University of Sydney, Australia (e-mail: yong.xia@sydney.edu.au; jwan5672@uni.sydney.edu.au; eberl@staff.usyd.edu.au; michael.fulham@sydney.edu.au; feng@it.usyd.edu.au).

Y. Xia, S. Eberl, and M. Fulham are also with the Department of PET & Nuclear Medicine, Royal Prince Alfred Hospital, Sydney, Australia.

M. Fulham is also with the Sydney Medical School, The University of Sydney, Australia.

D. Feng is also with the Center for Multimedia Signal Processing (CMSP), Department of Electronic & Information Engineering, Hong Kong Polytechnic University, Hong Kong, and also with the Med-X Research Institute, Shanghai JiaoTong University, China.

II. METHOD

A. Data Acquisition

We used 26 clinical brain FDG PET-CT studies, which had corresponding clinical MR (1.5T) data. All PET-CT studies were acquired on a Biograph LSO Duo PET-CT scanner 45 min after injection of 350 MBq of 18F-FDG. PET data were interpolated such that both PET and CT data had a dimension of $512\times512\times47$ and a voxel size of $0.49\times0.49\times3.4$ mm3. Each MR image was aligned to the corresponding CT image by using the SPM8 package [9], and then segmented into GM, WM and CSF by using the EMS package [16].

B. Probabilistic Brain Atlas Construction

We built the probabilistic brain atlas for each testing PET-CT image that was to be segmented from a set of 25 training cases, each of which comprised co-aligned PET data, CT data and segmented MR data. The transformation that mapped each training CT data to the testing CT data was estimated using the SPM8 package, and then applied to the segmented MR data. The spatially normalized MR segmentation results of all training cases were finally averaged and defined as the probabilistic brain atlas. For a PET-CT image with N voxels and K target regions, the probabilistic atlas is a matrix with $N\times K$ elements, and each element P_{nk} represents the anatomical knowledge provided by training cases on the prior probability of voxel n belonging to a particular tissue class k.

C. Segmentation Model

A brain PET-CT image is denoted by a set of 2D vectors $X=\{x_n;n=1,2,\cdots,N\}$, where $x_n=(HU_n,SUV_n)$ is the combination of the Hounsfield unit (HU) at voxel n in CT data and the standardized uptake value (SUV) at voxel n in PET data. Each voxel has a latent class label vector z_n comprising a 1-of-K binary vector with component $z_{nk}=1$ representing that voxel n belongs to tissue type k. The assembly of latent class labels gives an admissible segmentation result $Z=\{z_n;n=1,2,\cdots,N\}$.

We assumed that the vectors of the voxels from each of K brain tissue types can be modeled by a Gaussian distribution $N(\mu_k,\Lambda_k^{-1})$. The prior probability of each x_n being sampled independently from the k th Gaussian component was denoted by π_{nk}. Different from the traditional GMM, the prior probabilities in our model vary spatially with voxel locations and were predetermined by the probability brain atlas. Adopting the variational Bayes inference [15], we further assumed other Gaussian distribution parameters $\Theta=\{\mu_k,\Lambda_k;k=1,2,\cdots,K\}$ to be random variables following the independent Gaussian-Wishart distribution.

$$p(\Theta)=\prod_{k=1}^{K}\mathrm{N}\left(\mu_k;m_k^0,(\beta^0\Lambda_k)^{-1}\right)W(\Lambda_k;\nu^0,W_k^0) \tag{1}$$

where $\{m^0,\beta^0,\nu^0,W^0\}$ are hyper-parameters.

To estimate the MAP solution for image segmentation, we introduced a variational distribution $q(Z,\Theta)$ to infer the posterior distribution $p(Z,\Theta|X)$. For any choice of $q(Z,\Theta)$, the following decomposition holds [15]

$$\ln p(X)=KL(q\|p)+L(q) \tag{2}$$

with

$$KL(q\|p)=-\int\int q(Z,\Theta)\ln\frac{p(Z,\Theta|X)}{q(Z,\Theta)}dZd\Theta \tag{3}$$

$$L(q)=\int\int q(Z,\Theta)\ln\frac{p(X,Z,\Theta)}{q(Z,\Theta)}dZd\Theta \tag{4}$$

Since the log-likelihood $\ln p(X)$ is a constant for the observed image X, maximizing $L(q)$ is equivalent to minimizing the Kullback-Leibler (KL) divergence between $q(Z,\Theta)$ and $p(Z,\Theta|X)$. Consequently, the variational distribution $q(Z,\Theta)$ that maximizes $L(q)$ will be an approximation to the posterior distribution $p(Z,\Theta|X)$. With the assumption that $q(Z,\Theta)$ can be factorized between the latent variables Z and distribution parameters Θ, this maximization problem can be solved by using the variational EM (VEM) algorithm [15].

D. Segmentation Algorithm

Although our method differs from traditional inference of GMM in the assumptions regarding the prior probability of each voxel and the use of the prior anatomical knowledge in probabilistic brain atlas, the posterior distribution $p(Z,\Theta|X)$ can still be inferred in line with the VEM algorithm [15]. Our PA-VEM segmentation algorithm can be summarized as follows.

Step 1: Initialize the prior probabilities $\pi_{nk}=P_{nk}$, expectations $r_{nk}=P_{nk}$, and hyper-parameters: $\beta^0=0.1$, $m_k^0=\bar{x}_k$, $(W_k^0)^{-1}=S_k$, and $\nu^0=2$.

Step 2: Calculate synthetic statistics:

$$\begin{cases} N_k=\sum_{n=1}^{N}r_{nk} \\ \bar{x}_k=\frac{1}{N_k}\sum_{n=1}^{N}r_{nk}x_n \\ S_k=\frac{1}{N_k}\sum_{n=1}^{N}r_{nk}(x_n-\bar{x}_k)(x_n-\bar{x}_k)^T \end{cases} \tag{5}$$

Step 3: Calculate hyper-parameters:

$$\begin{cases} \beta_k=\beta^0+N_k \\ m_k=\frac{1}{\beta_k}(\beta^0m_k^0+N_k\bar{x}_k) \\ W_k^{-1}=(W_k^0)^{-1}+N_kS_k+\frac{\beta^0N_k}{\beta^0+N_k}(\bar{x}_k-m_k^0)(\bar{x}_k-m_k^0)^T \\ \nu_k=\nu^0+N_k \end{cases} \tag{6}$$

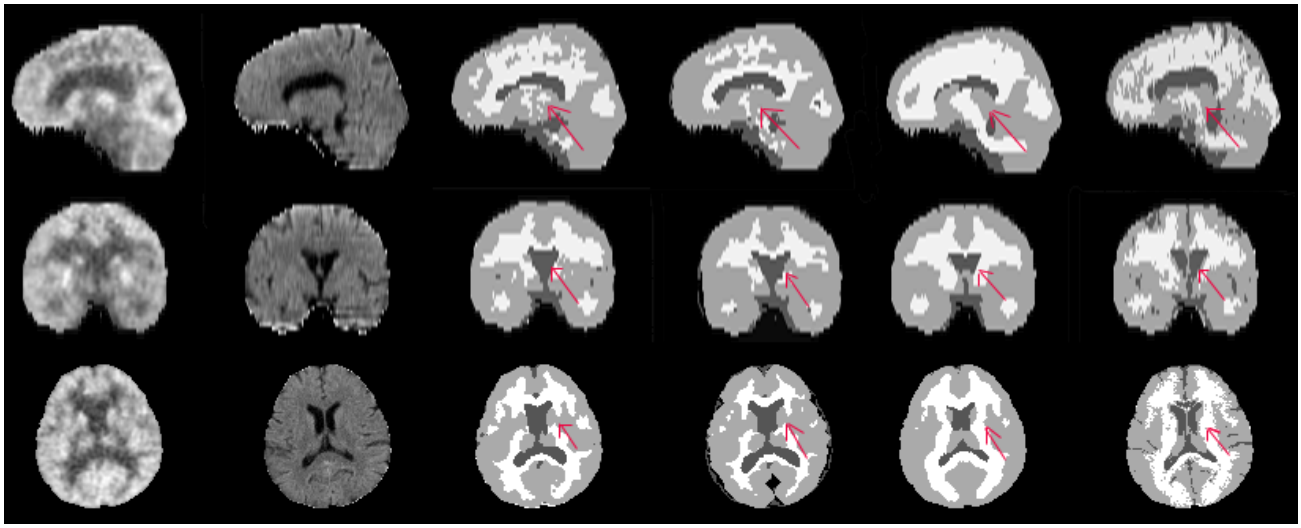

Fig. 1 The 235th sattigal slice, 240th coronal slice and 21st transaxial in one PET-CT study #16 (1st and 2nd columns), their segmentation results obtained by applying the EMS package (3rd column), SPM8 package (4th column), and PA-VEM algorithm (5th column), and the ground truth (6th column)

Step 4: Calculate the expectation of z_{nk}:

$$E[r_{nk}] = r_{nk} = \frac{\rho_{nk}}{\sum_{j=1}^{K} \rho_{nj}} \tag{7}$$

where

$$\ln \rho_{nk} = \ln \pi_{nk} + \frac{1}{2} E[\ln \det(\Lambda_k)] - \ln(2\pi) - \frac{1}{2} E_{\mu_k,\Lambda_k}\left[(x_n - \mu_k)^T \Lambda_k (x_n - \mu_k)\right] \tag{8}$$

Step 5: To use the anatomical information to regularize the statistical segmentation, we linearly combined the probabilistic brain atlas with the intermediate segmentation result as follows

$$r_{nk} = \lambda P_{nk} + (1-\lambda) r_{nk} \tag{9}$$

Step 6: If the number of iteration reaches 25 or the number of changed labels is less than 100, stop the segmentation process; otherwise, go to step 2.

E. Validation

We adopted the leave-one-out cross validation scheme, using one case each time for testing and the other 25 cases for training. For training cases, the GM, WM and CSF segmented from MR images were used to construct the probabilistic brain atlas, and for testing cases those MR segmentation results were used as an approximation of the ground truth. We compared the proposed PA-VEM segmentation algorithm to the segmentation methods in the EMS and SPM8 packages.

The ability of each algorithm to delineate each brain tissue type was assessed by using the Dice similarity coefficient (DSC) [17]. The accuracy of segmenting the entire brain was measured by the percentage of correctly classified voxels.

TABLE I
MEAN ± STANDARD DEVIATION OF SEGMENTATION ACCURACY OF THREE ALGORITHMS

Algorithms	SPM8	EMS	PA-VEM
DSC of GM (%)	75.6±4.0	78.5±4.1	80.1±4.8
DSC of WM (%)	56.6±4.6	64.3 ±4.1	70.1±5.7
DSC of CSF (%)	46.6±5.5	41.6±6.2	44.7±4.9
Overall Accuracy (%)	67.3±4.2	70.6±4.4	74.2±5.1

III. RESULT

The segmentation results of the 235th sagittal slice, 240th coronal slice and 21st transaxial slice from one PET-CT study (case 16) obtained by using the EMS package, SPM8 package and our PA-VEM algorithm are shown in Figure 1. The EMS and SPM8 packages result in obvious under-segmentation of WM, whereas our algorithm can produce results that are much more similar to ground truth. The mean and standard deviation of the three algorithms' segmentation accuracy in the 26 clinical cases are shown in Table I. It is evident that the proposed PA-VEM algorithm substantially improves the accuracy of brain PET-CT image segmentation, particularly in the delineation of WM.

IV. DISCUSSION

In statistical segmentation approaches, voxel values are modeled by the GMM with constant parameters, which are usually determined according to the maximum-likelihood criterion via the EM algorithm. However, the EM algorithm is intrinsically susceptible to over-fitting and local optimum convergence. We replaced the maximum-likelihood estimation with the variational Bayes inference, where model parameters were viewed as random variables, and hence

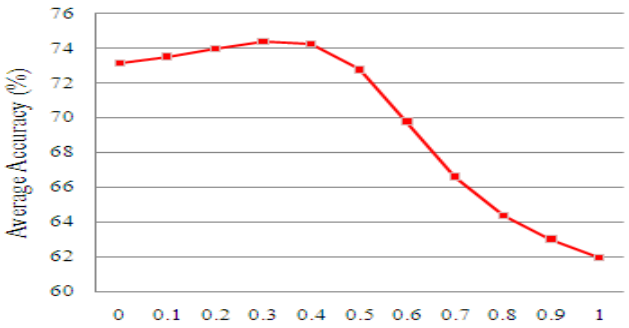

Fig.2. The variation of segmentation accuracy versus the value of the combination coefficient λ

increased the segmentation algorithm's flexibility.

Meanwhile, traditional statistical segmentation algorithms rely only on voxel values, and may result in noise-related artifacts, especially in PET-CT images where the noise can be large. We abandoned the unified prior mixing coefficients and allowed voxels to have different prior probabilities of belonging to all classes. To incorporate the prior anatomical information into the segmentation process, we used the probabilistic brain atlas not only to initialize the prior probabilities and other parameters, but also to regularize each intermediate result. Thus, the proposed PA-VEM algorithm is more suitable than other statistical approaches for brain PET-CT image segmentation.

In our algorithm, the combination coefficient λ plays a pivotal role in balancing the contribution of the prior anatomical knowledge and observed image information to the segmentation process. A smaller λ allows the image data to dominate the segmentation process, whereas a larger λ gives the probabilistic atlas more weight. The average segmentation accuracy in all cases versus the values of λ is plotted in Fig. 3. It shows that the accuracy of our algorithm is not sensitive to the choice of λ, when $\lambda \le 0.5$. The results presented in Fig. 1 and Fig. 2 were generated by setting λ to 0.3, which according to our trial experiments can produce good segmentation accuracy.

It is generally recognized that delineating brain tissues in PET-CT image is challenging, since those images have low spatial resolution, low contrast and high noise level. Hence, using the probabilistic brain atlas is essential to solve such segmentation problem. However, constructing a probabilistic atlas for each to-be-segmented study involves registration of multiple training cases to that study, which is time consuming. This is a major drawback of the proposed algorithm. Our future work will focus on fast and efficient atlas construction.

V. Conclusion

We have proposed the PA-VEM algorithm to delineate GM, WM, and CSF regions from clinical brain PET-CT images. We found that our algorithm substantially improves the segmentation accuracy when compared to the segmentation approaches in the widely used EMS and SPM8 packages.

References

[1] J. R. Petrella, et al., "Neuroimaging and early diagnosis of Alzheimer Disease: A look to the Future," Radiology, vol. 226, pp. 315-336, 2003.
[2] H. D. Protas, et al., "Regional quantitative analysis of cortical surface maps of FDG PET images," presented at the IEEE Nuclear Science Symposium Conference Record (NSS'05), 2005.
[3] G. J. Topping, et al., "Methods for Parkinson's Rat Model PET Image Analysis with Regions of Interest," presented at the IEEE Nuclear Science Symposium Conference Record (NSS '07), 2007.
[4] P. Raniga, et al., "Spline Based Inhomogeneity Correction for 11C-PIB PET Segmentation Using Expectation Maximization," presented at the International Conference on Medical Image Computing and Computer Assisted Intervention (MICCAI 2007), Brisbane, Australia, 2007.
[5] J. Tohka, et al., "Genetic algorithms for finite mixture model based voxel classification in neuroimaging," IEEE Transactions on Medical Imaging, vol. 26, pp. 696-711, May 2007.
[6] J. Mykkanen, et al., "Automatic extraction of brain surface and mid-sagittal plane from PET images applying deformable models," Computer Methods and Programs in Biomedicine, vol. 79, pp. 1-17, 2005.
[7] P. Raniga, et al., "PIB-PET segmentation for automatic SUVR normalization without MR information.," in IEEE International Symposium on Biomedical Imaging: From Nano to Macro (ISBI 2007), Washington, DC, USA, 2007, pp. 348-351.
[8] J. Ashburner and K. J. Friston, "Unified segmentation," Neuroimage, vol. 26, pp. 839-851, 2005.
[9] Members and collaborators of the Wellcome Trust Centre for Neuroimaging, Institute of Neurology, University College London, 2009, Statistical Parametric Mapping (SPM5). Available: http://www.fil.ion.ucl.ac.uk/spm/
[10] V. Potesil, et al., "Automated tumor delineation using joint PET-CT information," presented at the SPIE Medical Imaging 2007: Computer-aided Diagnosis, 2007.
[11] Y. Xia, et al., "Segmentation of brain structures using PET-CT images," presented at the International Conference on Technology and Applications in Biomedicine (ITAB 2008), Shenzhen, China, 2008.
[12] Y. Xia, et al., "Segmentation of dual modality brain PET/CT images using the MAP-MRF model," in 2008 IEEE 10th Workshop on Multimedia Signal Processing (MMSP 2008), Cairns, Queensland, Australia, 2008, pp. 107-110.
[13] Y. Xia, et al., "Segmentation of Brain PET-CT Images Based on Adaptive Use of Complementary Information," presented at the SPIE Medical Imaging 2009: Image Processing, 2009.
[14] Y. Xia, et al., "Dual-modality 3D brain PET-CT image segmentation based on probabilistic brain atlas and classification fusion," presented at the ICIP'10, 2010.
[15] C. M. Bishop, Pattern Recognition and Machine Learning, 2nd ed. New York: Springer, 2007.
[16] K. Van Leemput, et al., "A unifying framework for partial volume segmentation of brain MR images," IEEE Transactions on Medical Imaging, vol. 22, pp. 105-119, 2003.
[17] A. P. Zijdenbos, et al., "Morphometric analysis of white matter lesions in MR images: method and validation," Medical Imaging, IEEE Transactions on, vol. 13, pp. 716-724, 1994.